ELSEVIER

Journal of Nuclear Materials 244 (1997) 273–277

journal of nuclear materials

Metastable reversal of the martensitic phase in Nb_3Sn induced by energetic-electron irradiation [1]

C.L. Snead Jr. [a,*], R.C. Birtcher [b], M.A. Kirk [b]

[a] *Department of Advanced Technology, Brookhaven National Laboratory, Upton, NY 11973-5000, USA*
[b] *Materials Science Division, Argonne National Laboratory, Argonne, IL 60439, USA*

Received 29 August 1996; accepted 28 October 1996

Abstract

Nb_3Sn upon cooling undergoes a structural martensitic phase transition from the cubic A-15 structure to a tetragonal one commencing at about $T_m = 50$ K, with the c/a of the tetragonal structure increasing as the temperature is decreased until the ratio becomes constant at the superconducting transition temperature T_c. During electron irradiations between 0.4 and 2.0 MeV the electrical resistivity at 20 K initially *decreased*, contrary to experience with irradiated metals. For electron energies above the energy determined to be threshold for the production of Frenkel defects the resistivity eventually increased with increasing dose as expected. For energies below threshold, however, the resistivity approached a limiting value of about 99.6% of the initial resistivity before irradiation. The resistivity vs. temperature shows a deviation to higher-resistivity values as temperature is lowered commencing at T_m with increasing deviation as the tetragonality increases at lower temperatures. We ascribe the observed decrease in resistivity with electron irradiation to a metastable reversal of the tetragonal phase toward a state of reduced tetragonality (to cubic). This resistivity decrease is completely recovered in annealing to slightly above T_m. High-voltage electron microscopy at 12 K confirms the decrease in tetragonality by a disappearance of the twin boundaries associated with the tetragonal phase. The microstructure responsible for the resistivity changes will be discussed.

1. Introduction

The influence of point defects on the superconducting critical properties and also the mechanical properties of the type-II A15 superconductors is quite significant [1–3]. Of particular importance is the structural disorder induced by radiation damage. This disorder is usually characterized as 'antisite' defects caused by $A \leftrightarrow B$ interchange in the disordered A_3B lattice. We report here an anomalous radiation-induced *decrease* in the normal-state resistivity of Nb_3Sn when irradiated by electrons below T_c (~ 18 K) at energies above and below the threshold for atomic displacement. This observation was made during studies of the displacement damage threshold and post-irradiation recovery phenomena reported elsewhere [4].

2. Experiment

Thin films of Nb_3Sn were deposited by co-evaporation on 0.0125-cm-thick sapphire substrates. The film was masked and the desired specimen geometry produced by sand blasting. Four resistivity specimens in series with probes for attaching leads were produced. One of these specimens was separated from the ones to be irradiated by 0.5 cm and was used as a calibration specimen. All of the specimens were connected in series. From the measured sample thickness of 2.5×10^{-5} cm and a length-to-area ratio of 8×10^4 cm^{-1}, a normal-state resistivity at 20 K of ~ 10 $\mu\Omega$ cm is deduced.

The four-probe resistance measurements were accomplished using a data-acquisition system composed of a Guildline 7.5-digit voltmeter, an Accurex Autodata Scan-

* Corresponding author.

[1] Work performed under the auspices of the Basic Energy Sciences Division of the Department of Energy under Contract No. DE-AC02-76CH00016.

PII S0022-3115(97)00004-4

ner, North Hills precision dc power supply, and a MINC-II computer. All resistance measurements were made at 20 K. Typically five resistance measurements were performed during an irradiation at a given energy. At least 30 determinations of each of the three specimens were made for both forward and reversed current. Since the temperature drifted a few hundredths of a Kelvin during the measurements, a least-squares fit to a straight line through the R vs. temperature data allowed a value at a 'standard' temperature to be determined. This procedure was necessitated by the fact that at 20 K, the base temperature selected about 2 K above the critical temperature, the resistivity changes very rapidly with changing temperature. The base temperature of 20 K was chosen to minimize the slope of the resistivity vs. temperature for more accurate resistivity determinations but also to be far enough above T_c so as to avoid superconducting fluctuations.

The irradiations were performed in a standard liquid-helium cryostat with electrons supplied by the Brookhaven Dynamitron accelerator. The beam was rastered over a water-cooled copper collimator with only the middle 20% of the beam center on target to achieve uniformity. The beam current on target was typically 4 μA, and the spot size was 0.26 cm^2. The resulting typical electron flux was 9.7×10^{17} e/m^2 s. Irradiations and resistivity-change measurements were performed at several energies from 0.4 to 2.0 MeV.

For the TEM investigation performed at the Argonne High Voltage Electron Microscope Facility the Nb_3Sn sample was furnace grown, cut, and electropolished [5]. Micrographs were taken in a small [110] normal grain. The electron irradiation direction was about 6° from [110] (avoiding channeling). The electron energy was 700 keV and micrographs were also taken at this energy. This TEM experiment was part of a larger independent investigation of the low-temperature martensitic transformation [6], in which this energy was selected to be just below what was thought to be the threshold to displace atoms. The sample temperature was 12 K. Temperature rise under the electron beam had been measured by observing temperature-sensitive changes in the martensite structure, and was estimated to be < 2 K. Electron current density was measured by Faraday cup to be 1.56×10^{23} e/m^2 s on the sample.

3. Results

Nb_3Sn undergoes a martensitic phase transition from the cubic A-15 to the tetragonal structure upon cooling with the transition temperature T_m at about 50 K. As the temperature is further reduced below T_m, the tetragonality of the lattice increases monotonically until further change is arrested at the superconducting transition temperature, around 18 K. This phase transformation is nicely depicted [5] in Fig. 1 in which the internal friction is plotted as a function of temperature for a Nb_3Sn film. The martensitic

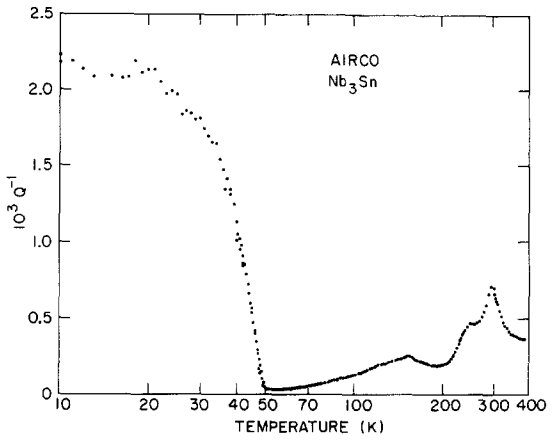

Fig. 1. The internal friction of Nb_3Sn as a function of temperature. The friction due to domain-wall motion associated with the martensitic phase below 50 K is featured.

phase transition onset, T_m, is well delineated near 50 K as is the superconducting cutoff of the increase in tetragonality at 18 K (T_c). The internal friction is caused by the stress-induced motion of the boundary walls between adjacent tetragonal domains. The functional change of the internal friction can be fit by an expression involving the square of the anisotropy ratio, c/a, with the maximum tetragonal distortion producing a c/a of about 1.0001. This fit is seen [7] in Fig. 2. This increasing tetragonality with decreasing temperature is manifested also in an increasing resistivity contribution at lower temperatures from electron scattering from the growing domain boundaries (twins).

We have measured the resistance of the Nb_3Sn irradia-

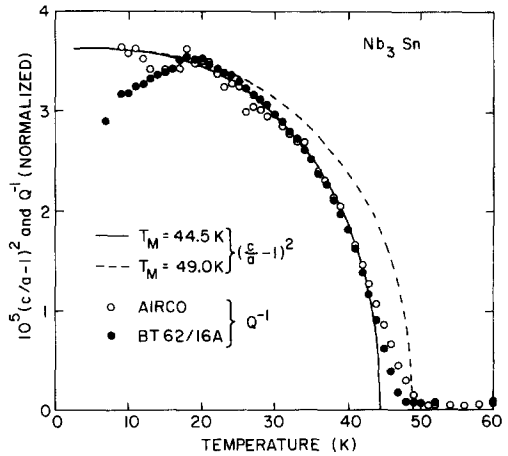

Fig. 2. A fit to the internal friction where the dominant term is the tetragonality squared is shown for two specimens of Nb_3Sn. The magnitude of the internal friction of the two specimens is normalized at 18 K. 'Airco' designates the company from which the tapes were obtained.

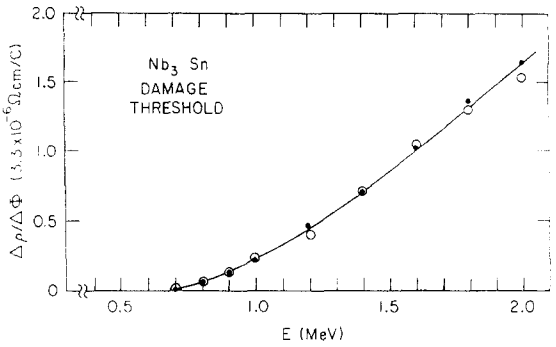

Fig. 3. The resistivity change per unit fluence for various electron energies. The energy deduced from the intercept point on the energy axis, used in Eq. (1), allows the determination of the threshold energy for the production of Frenkel defects.

tion specimens over this same temperature range. It is clear that a break in the data occurs at 50 K, with the slope of the curve below T_m indicating a slower decrease in the resistance as the temperature is lowered than what would have been for a projection of the curve obtained above T_m in the cubic phase. It is concluded that the anisotropy of the tetragonal-phase material produces a higher-resistivity material at 20 K than would have eventuated if the material had remained cubic. Presumably, phase boundaries would contribute to an increased electron scattering, and thus produce a higher resistivity.

The original purpose of this research was to use low-temperature electron irradiation to establish the threshold damage energy for the production of Frenkel defects. This was to be followed by isochronal annealing to above room temperature so as to establish the recovery stages. The threshold energy is obtained by performing irradiations at different energies, establishing a linear increase of the resistivity with increasing fluence as the Frenkel defects are being created (assumed to be immobile at temperatures below 20 K), and plotting $\Delta\rho/\Delta\Phi$ vs. incident electron energy. Damage threshold is then defined as the point where $\Delta\rho/\Delta\Phi$ intersects the energy axis. Using the value of the intercept in the expression

$$E_p(\max) = 2E(E + 2mc^2)/Mc^2, \quad (1)$$

where E and m are the energy and mass of the incident electron, and M is the (averaged) mass of the lattice atom.

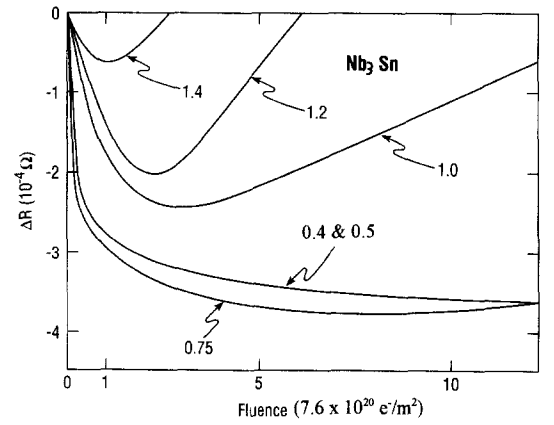

Fig. 4. The change in resistance in Nb_3Sn as a function of electron fluence for several incident electron energies. To be noted are the negative value of the resistance change, the fact that resistance changes are evident below threshold energy for the production of Frenkel defects (0.75 MeV), and the saturation of the resistance decrease for those energies. Note that the value for the fluence on the abscissa at the number 10 corresponds to 7.6×10^{17} e/cm^2.

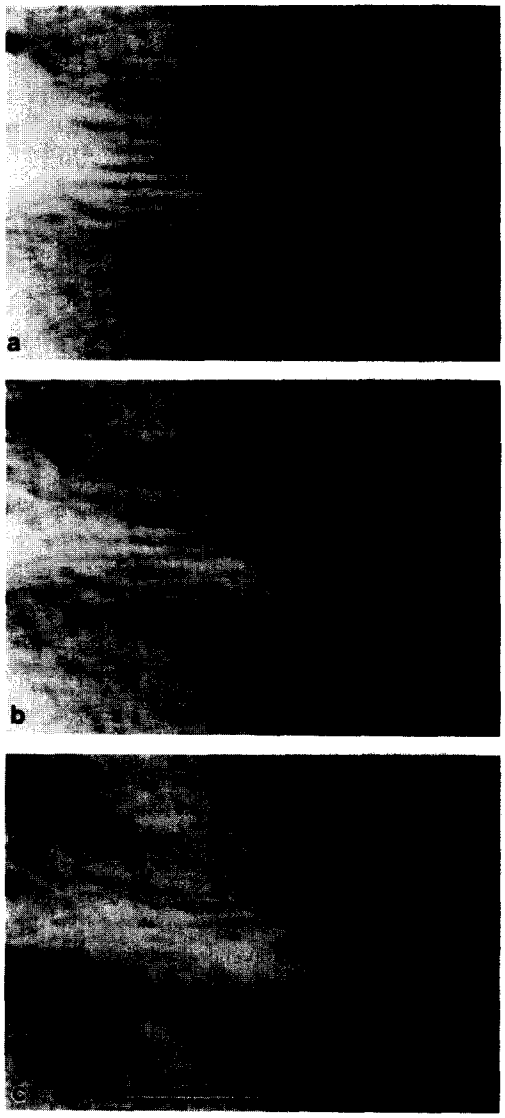

Fig. 5. Three micrographs stacked vertically. The time of exposure to the electron beam is 10, 60, and 120 s, top to bottom. The size bar shown in (c) is representative for all three micrographs and represents a length scale of 300 nm.

The plot is shown in Fig. 3 where the intercept energy of 0.7 MeV produces a threshold energy [E_p(max)] of 27.4 eV. This value is very similar to that reported for pure Nb of 28 eV [8].

During the accumulation of the production data at various energies an anomaly was noted. Instead of getting the expected monotonic (linear) increase in resistivity as defects are produced in the lattice, in many cases the initial change in the resistivity was a *decrease*. Upon closer scrutiny of the earliest stages of the various irradiations it was found that: (1) the behavior was initially a decrease that diminished and eventually became the linear increase as expected for electron energies above what was to be determined as the threshold energy, (2) the magnitude of the total decrease observed increased with decreasing electron energy, (3) the decrease occurred for electron energies well below the threshold energy for Frenkel pair production, and (4) below threshold the resistivity decrease approached a saturation or limiting value with increasing fluence. This behavior is plotted in Fig. 4 where the change in resistance is plotted vs. dose for electron energies ranging from 0.4 to 1.4 MeV.

The results of the transmission microscopy are presented in three micrographs in Fig. 5. Micrograph (a) of one grain after 10 s of irradiation at 700 keV at 12 K clearly shows the twin-boundary structure that is the signature of the martensite material. In micrograph (b) after 60 s of irradiation the boundaries have faded significantly, while in micrograph (c) only vestiges of the twin-boundary structure can be observed. Two other qualitative observations include: there were no other signs of electron damage (small clusters of point defects); similar fading of martensite structure was seen in other grains, but the time to fade varied, suggesting possible orientation dependence.

4. Discussion and conclusions

From the behavior of the changes observed in the electrical resistivity in Nb after irradiation at various energies (Fig. 4), we conclude that there are two mechanisms associated with the electron irradiation. The first is the standard increase due to Frenkel-pair production which is seen above 700 keV (threshold energy). The second mechanism caused a decrease in the resistivity as a function of fluence. This decrease is seen for all irradiations, but is more pronounced for electron energies below the threshold energy where the Frenkel-pair contribution is not present. The resistivity decrease is seen to saturate at a level of about -3.8 (about 0.4% of R_0) on the scale shown for the below threshold irradiations. Indeed, for two competing mechanisms with one saturating, the saturation value can also be estimated by extrapolating the higher-fluence data for the energies above threshold back to the ordinate where the intercept gives the saturation value for the mechanism causing the decreases. (This assumes Frenkel-pair production provides a linear increase in electrical resistivity over these fluences at this temperature.) For instance, define the saturation decrease to be about -3.7 in Fig. 4 based upon the high-fluence values for the 0.4, 0.5, and 0.75 MeV. Laying a straight edge on the higher-fluence linear portion of the curves for the 1.0 and 1.2 MeV data, the ordinate intercept is at (or near) the -3.7 value. (The data for the 1.4-MeV curve do not extend far enough to define well a higher-fluence linear behavior.)

No observations of decreases in electrical resistivity in monatomic metals as a consequence of energetic particle irradiation have been made to our knowledge. Decreases have been observed in ordering alloys where enhanced diffusion owing to the migration of the vacancy member of Frenkel pairs produce enhanced order over that prior to irradiation. In the case here, however, the decreases are seen for irradiations below the Frenkel-pair production threshold, indicating that what is being observed is due to a diffusionless process. This fits our interpretation as to what the mechanism involved is attributable. The martensitic phase transformation in Nb_3Sn is a classical diffusioness transformation from the cubic structure to tetragonal, with a resulting increase of resistivity in the tetragonal phase due to electron scattering from the twin boundaries that are produced owing to the tetragonal nature of the low-temperature phase. The reversal of the transformed material metastably back toward the cubic phase by electron irradiation at 20 K therefore results in the decrease in electrical resistivity observed. We annealed the specimen irradiated at 0.5 MeV to 60 K and remeasured the resistivity at 20 K. The resistivity decrease due to the irradiation was found to recover completely as a result of this anneal above T_m, consistent with our interpretation.

The TEM results on Nb_3Sn depicted in the micrographs of Fig. 5 are interpreted as a beam-induced reduction of the tetragonal phase of the material as evidenced by the disappearance of the tetragonal phase twin boundaries. Although the beam energy is now known to be very near the threshold to produce displaced atoms, we believe the microscopy result is at least suggestive of a subthreshold mechanism consistent with the decrease in resistivity. The general fading of the twin boundaries under irradiation is indicative of a relief of the strain energy by reversion of the tetragonal structure to the cubic structure, rather than a conversion of the two twinned orientations into one, thus retaining the tetragonal structure. To be entirely convincing, the microscopy experiment should be performed at energies significantly below threshold, as was part of the resistivity experiment. In the same vein any differences between irradiation at 12 and 20 K should be investigated, although such differences seem unlikely. The TEM results are for irradiation and micrographs taken at 12 K, whereas the electrical resistivity results were for irradiations below 20 K and measurements at 20 K.

While we are sure of what is going on as a result of the irradiations, the basic mechanism bringing about the phase

reversion is not so clear. We can at present only speculate on what microscopic mechanisms may be operative in transferring beam energy to metastable lattice configurations. The primary energy loss of electrons passing through a metal is electron scattering. One can envision an electron–phonon interaction transferring the deposited energy to the lattice atoms and creating an analog to the thermal spike generated in energetic neutron irradiation. The quenching of the spike zone could then be seen as causing the metastable cubic phase to be 'frozen in'. Simple dE/dx calculations do not seem to provide sufficient energy over enough atomic volumes to make this mechanism viable.

The other major energy-loss path is through elastic scattering of the electrons from nuclei. The damage energy imparted by the electron to the primary knock-on atom is partitioned between energy required to displace atoms to interstitial sites (above threshold) and vibrational energy distributed among interacting lattice atoms. For below-threshold irradiations, all of the damage energy will go into the latter channel. In order to bring about the phase reversion, one then attributes the energy of vibration to allow the atoms to be displaced sufficiently from their equilibrium lattice positions that they occupy in the tetragonal phase such that they can end up on their cubic sites when the energy is dissipated. Since the distortion from the tetragonality of the lattice is small (about 0.001 strain), sufficient damage energy will be available from a single electron collision to provide vibrational energy to many lattice atoms sufficient to produce displacement distances sufficient to span the tetragonal and cubic lattice positions. Furthermore, the dense packing of the Nb A-chains along the $\langle 100 \rangle$ directions would make it possible for long chains of atoms to be affected through the focusing mechanism from single energy-transfer events.

At this point we feel that the basic interaction responsible for the observations as discussed above is still quite speculative. Also, an apparent inconsistency arises in comparing the resistivity results with the TEM results. For the resistivity decreases portrayed in Fig. 4, saturation is seen to occur for 0.4, 0.5, and 0.75 MeV between $(5–10) \times 3 \times 10^{-3}$ C $(3.8–7.6) \times 10^{17}$ e/cm^2. In the electron-microscopy results portrayed in Fig. 5, the twin-boundary structure is still visible at 60 s of irradiation corresponding to a fluence of 9×10^{20} e/cm^2, a more than three order of magnitude difference. While the measuring temperatures for the two techniques was different, and some variation in fluence for the disappearance of the twin structure was observed for different grain orientations, this large difference remains puzzling. Another possibility is that the difference in required dose might be attributable to a strong surface effect [9] in the much thinner TEM sample by which the surfaces serve to maintain the tetragonal phase, thus requiring larger electron exposure to destabilize the structure.

Acknowledgements

Thanks go to Arup Ghosh for providing the samples and to W. Tremel for managing the data acquisition.

References

[1] A.R. Sweedler, D.G. Schweitzer and G.W. Webb, Phys. Rev. Lett. 33 (1974) 168.
[2] B.S. Brown, J. Nucl. Mater. 97 (1981) 1.
[3] C.L. Snead, Jr. and T. Luhman, in: Physics of Radiation Effects in Crystals, eds. R.A. Johnson and A.N. Orlov (Elsevier, Amsterdam, 1986) p. 345.
[4] C.L. Snead, Jr., in: 16th National SAMPE Technical Conference, Hi-Tech Review 1984, Vol. 16 (Society for the Advancement of Material and Process Engineering) p. 228.
[5] M.A. Kirk, M.C. Baker, B.J. Kestel, H.W. Weber and R.T. Kampwirth, Effects of Radiation on Materials, Standard Technical Publication 1046 (1990) pp. 587–595.
[6] M.A. Kirk and B. Kestel, to be published.
[7] C.L. Snead, Jr. and D.O. Welch, J. de Phys. Coll. C10, Tome 46 (1985) C10–589.
[8] P. Jung and G. Lucki, Rad. Effects 26 (1975) 99–102.
[9] R.A. Cowley and G. Shirane, J. Phys. C: Solid State Physics 11 (1978) L939.